Available online at www.sciencedirect.com
SCIENCE DIRECT
Tetrahedron
ELSEVIER
Tetrahedron 62 (2006) 4162–4172

Chiral discrimination of ibuprofen isomers in β-cyclodextrin inclusion complexes: experimental (NMR) and theoretical (MD, MM/GBSA) studies

Carlos-Javier Núñez-Agüero,[a] Carolina-Marta Escobar-Llanos,[b] David Díaz,[b] Carlos Jaime[c] and Ramón Garduño-Juárez[d,*]

[a]*Centro de Investigaciones Químicas, Universidad Autónoma del Estado de Morelos, Ave. Universidad 1001, 62210 Cuernavaca, Morelos, México*
[b]*Facultad de Química, Universidad Nacional Autónoma de México, Coyoacán, 04510, México D.F., México*
[c]*Departamento de Química, Universidad Autónoma de Barcelona, 08193 Bellaterra, Spain*
[d]*Centro de Ciencias Físicas, Universidad Nacional Autónoma de México, Apdo. Postal 48-3, 62250 Cuernavaca, Morelos, México*

Received 22 October 2005; revised 20 January 2006; accepted 2 February 2006

Available online 9 March 2006

Abstract—In this paper, we analyze the energetic and conformational preferences involved in the chiral discrimination of ibuprofen (**Ibu**) isomers by beta-cyclodextrin (β-CD) when forming inclusion complexes in water. This study was performed by means of atomistic molecular mechanics simulations upon four different penetration modes of the guest, and a structural 2D NMR experiment. The trajectories of these simulations were treated with the MM/GBSA method in order to obtain the relative weights of the different free energy components. The resulting values of the free energy of binding and other geometrical features indicate that this chiral selectivity is influenced by a preferred penetration mode involving the *S*-(+)-**Ibu** isomer. The calculated $\Delta\Delta G$ of binding is in good agreement with published experiments.

1. Introduction

Chiral discrimination is one of the most intriguing phenomena in chemistry. It is of great importance in analytic, organic, and biological chemistry. Stereoselective recognition is the basis of asymmetric synthesis, chromatography techniques, enzymatic catalysis, and origin of the chiral composition of the molecules constituting biological systems.[1] Despite the fundamental importance of this effect, its origin and nature are still far from being well understood at the atomic level. Chiral cyclodextrin (CD) hosts have been used extensively as models for investigating chiral and molecular recognition. Solution studies of CD inclusion complexes[2,3] and binding constants,[4] have provided thermodynamic data useful for chromatographic applications.[5] However, despite intense efforts, the mechanism of the recognition is not fully understood and many essential data are missing.

In pharmacology chirality is an important factor in drug efficacy. About 56% of the drugs currently in use are chiral compounds, and about 88% of these chiral synthetic drugs are used therapeutically as racemates. Unfortunately, there are many racemic drugs where the stereospecificity of the metabolism and/or pharmacodynamic effect of the enantiomers is not known. Studying the chiral recognition by CDs is of considerable importance in view of its enantiodifferentiation of drugs. A large number of experimental[6–10] and theoretical works have been performed over the past few years on CDs drug complexes.[11–13]

Besides experimental measurements, it is possible to accurately estimate the free energy of binding ($\Delta G_{\text{binding}}$) between small druglike molecules and a larger target molecule using computer simulation methods. One way is to use the very CPU intensive methods like the free energy perturbation (FEP) and thermodynamic integration (TI) techniques. Another way is to use the MM-PBSA/GBSA method[14] that in the last decade has been applied successfully to estimate the binding free energies of different biological systems.[15,16] This approach combine molecular mechanics energies for the solute with a continuum solvation approach and normal mode analysis

Keywords: Inclusion complexes; β-Cyclodextrin; Chiral discrimination; Molecular modeling; Free energy analysis; Molecular recognition.
* Corresponding author. Tel.: +52 777 329 1749; fax: +52 777 329 1775; e-mail: ramon@fis.unam.mx

0040–4020/$ - see front matter © 2006 Elsevier Ltd. All rights reserved.
doi:10.1016/j.tet.2006.02.010

to evaluate the total free energy. Depending on whether the continuum solvation model is based in solving the Poisson–Boltzmann equation or the Generalized Born equation is called MM-PBSA or MM-GBSA. The MM-PBSA/GBSA method is faster by at least a factor of 10 than the traditional FEP and TI techniques. Furthermore, it does not require any experimental data or fitting of parameters, it calculates the free energies of the end states directly, avoiding the time-consuming simulation of intermediate states as in FEP and TI methods.[17]

Given that in the chiral recognition process the guest molecules being discriminated have the same size, same molecular charges, same physicochemical properties, etc. they can only be discerned when different diasteromeric responses take place when they associate with another chiral molecule. It is generally accepted that the intermolecular forces responsible for enantiomer discrimination are the same as those involved in other types of molecular recognition, although the differences in binding energies of the enantiomers are much smaller in magnitude. In spite of this belief the so called three-point interaction model[18–20] between one enantiomer and the chiral selector, and the induced fit effect on chiral discrimination must be studied in more detail.

In this study, we used β-cyclodextrin (β-CD) as the chiral host and the two ibuprofen (4-isobutyl-2-phenyl-propionic acid) isomers as the chiral guests. β-CD is a cyclic oligomer made of seven α-D-glucose residues arranged in a donut-shaped ring with a dipole moment of about 2.311 D. The specific coupling and conformation of these glucose units give the cyclodextrin a rather rigid, toroidal molecular structure with a hollow interior of specific volume. The lining of the cavity is formed by hydrogen atoms and glycosidic bridging oxygen atoms; consequently this surface is fairly hydrophobic. The unique shape and physical–chemical properties of the cavity allows the formation of inclusion complexes with organic molecules, where the extent of the complex formation depends on the polarity of the absorbed molecules. The hydrophilic characteristic of β-CD is provided by its two different rims: one narrower (N) or primary hydroxyl rim and another wider (W) or secondary hydroxyl rim. These features are shown in Figure 1. Ibuprofen (**Ibu**) is a drug molecule containing a single chiral center, a long non-polar (NP) chain and a polar (P) end; properties that are useful for constructing a simple and good model in which study chiral discrimination. **Ibu** is one of the most effective and widely used non-steroidal analgesic and anti-inflammatory agent. **Ibu** is a polar molecule with a dipole moment around 1.8 D (computed with PM3 method). It is marketed as a racemic mixture though it is known that the pharmacological activity resides in the *S*-(+)-**Ibu** (**Ibu***S*) enantiomer only. However, in vivo testing the presence of an isomerase can convert the *R*-(−)-**Ibu** (**Ibu***R*) to the active **Ibu***S* enantiomer. Complexes of **Ibu** with β-CD and modified β-CD have been reported.[21]

Most of the experimental studies around **Ibu** chiral separation have been carried out in aqueous solution using a large variety of techniques such as: fluorescence measurements,[22,23] differential scanning calorimetry,[24] crystallography,[25] capillary electrophoresis,[26] potentiometric studies,[27] spectroscopy,[28] and supercritical fluid chromatography.[29] In turn, the number of theoretical studies on the complexation of **Ibu** by β-CD are few. These include use of MC/SD,[27] simulated annealing,[30] AM1 semi-empirical calculations,[24] and semi-empirical PM3 calculations.[31] Both experimental and theoretical studies suggest that features such as guest fit to the CD cavity, solvent interactions, hydrogen bonding potential of the guest molecules, and van der Waals forces combine to play a significant role in chiral discrimination. However, none of those studies furnish data regarding the specific role of the enantiomeric interactions and the spatial arrangements involved in the chiral discrimination of the guest molecules.

This article describes the results of several 4.5 ns molecular dynamics simulations, carried out on four different penetration modes of the **Ibu** isomers into the β-CD cavity

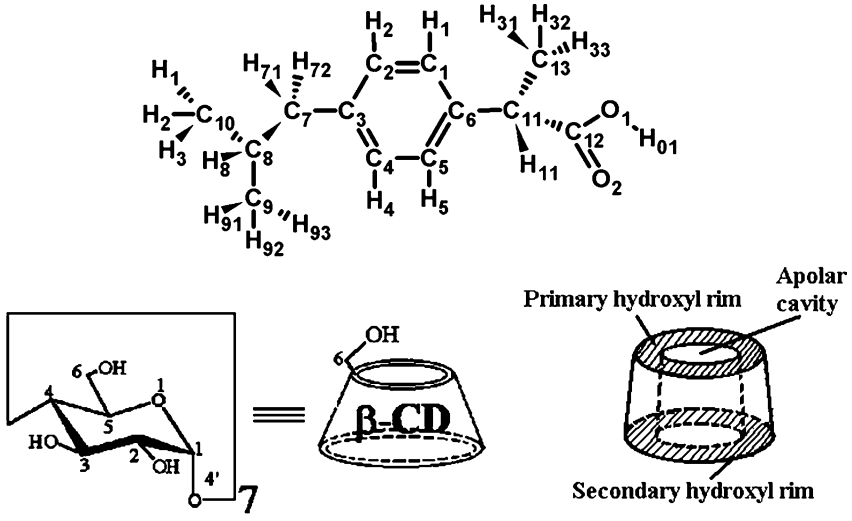

Figure 1. Structures of ibuprofen and β-CD.

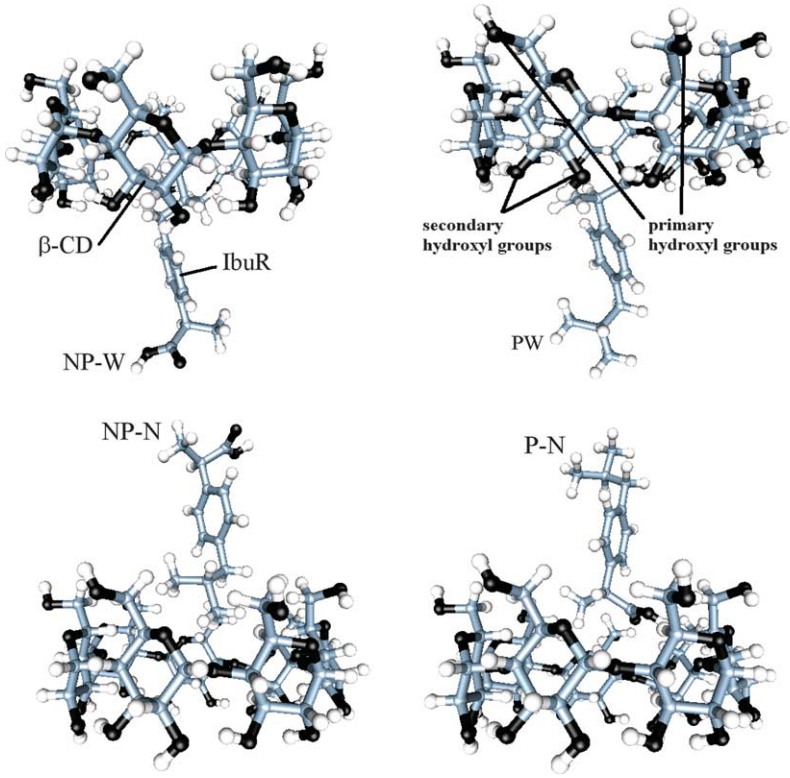

Figure 2. An schematic representation of the four different penetration modes of **Ibu** into β-CD. The corresponding minimized geometries are used as the starting points for the MD simulations.

in the presence of explicit solvent (Fig. 2). Detailed analyses of our results reveal that among the four penetration modes, there is one that appears to possess the most predominant discriminating features. During most of the simulation time, this penetration mode produces a large number of hydrogen bonds between the carboxyl group of **Ibu***S* and the secondary hydroxyl groups of β-CD. A trace analysis shows that for this penetration mode there are evident differences in occupancy and orientation between the two **Ibu** enantiomers inside the β-CD cavity, which in turn plays an important role in maximizing hydrogen bonding. The results of the remaining three penetration modes are also presented and we discuss how they contribute to the average $\Delta\Delta G_{\text{binding}}$ that facilitate the chiral discrimination of **Ibu** in a racemic mixture.

It is known that the carboxylic group of benzoic acid (BA) binds well within α-CDs,[32] especially in its non-ionized form, and that ionization of the carboxylic group leads to a much weaker binding.[33] Recent studies on the crystal structure of the inclusion complex of β-CD with BA show that the COOH groups of the BA molecules protrude at the β-CD O-6 sides,[34] and maintained in position by hydrogen bonding to the surrounding O-6-H groups. However, conflicting views are expressed in the literature regarding the stereoselectivity of inclusion of benzoic acid derivatives. Thus, in order to gain some extra information about the intermolecular interactions accompanying complexation we also report the results of association experiments via electronic absorption spectroscopy and a NMR 2D-NOESY study on complexes of the ionic form of ibuprofen ($\mathbf{Ibu}^{-1}$) with β-CD. We expected that NMR results would give structural information about the system by showing any particular interaction as a corresponding cross peak.

2. Results and discussion

2.1. MM/GBSA analysis

The results of the MM/GBSA analysis upon the 4.5 ns MD trajectories on the four penetration modes are gathered in Tables 1–3. In Table 1, we show the free energy contribution of the ligands alone. Solvation energies ($G_{\text{solvation}}$) for isolated **Ibu***R* and **Ibu***S* are identical for all arrangements (about −8.2 kcal/mol), however, small differences of about 1–4 kcal/mol are observed among the different conformers of β-CD (Table 1) and the respective complexes (Table 2). These results suggest that solvation by itself does not contribute significantly to the chiral selectivity; instead they suggest that chiral selectivity arises mainly from a delicate balance between internal energies. According to these calculated results, the complexes formed with the **Ibu***S* enantiomer are more stable than those for **Ibu***R*; however, if we consider the stability of the guests relative to the host we find that both the complex and the guest favor the [**Ibu***S*⊂β-CD] complex, while the host favors the [**Ibu***R*⊂β-CD] complex.

The results shown in Table 3 indicate that the initial arrangements P–W, NP–N and P–N have no clear chiral selectivity, while the initial orientation NP–W is responsible for a reasonable degree of enantioselectivity. Our

Table 1. Energy contribution of the ligands alone [**A** ≡ β-CD, **B** ≡ **Ibu**]

	Energy (kcal/mol)	NP–W_R (std)[a]	NP–W_S (std)	P–W_R (std)	P–W_S (std)	NP–N_R (std)	NP–N_S (std)	P–N_R (std)	P–N_S (std)
A	E_{electr}	439 (0.4)	446.3 (0.4)	444.3 (0.4)	438.0 (0.4)	441.9 (0.4)	441.7 (0.4)	443.3 (0.1)	445.1 (0.4)
	E_{vdW}	16.2 (0.2)	14.8 (0.2)	15.7 (0.2)	16.8 (0.2)	16.0 (0.2)	16.3 (0.2)	16.3 (0.2)	16.2 (0.2)
	$G_{(non\text{-}polar\ GB)}$	8.7 (0.0)	8.7 (0.0)	8.7 (0.0)	8.7 (0.0)	8.7 (0.0)	8.7 (0.0)	8.7 (0.0)	8.7 (0.0)
	G_{GB}	−71.5 (0.2)	−75.0 (0.2)	−75.0 (0.2)	−71.3 (0.2)	−72.3 (0.2)	−76.3 (0.2)	−73.1 (0.3)	−75.4 (0.2)
	$G_{solvation}$	−62.8 (0.2)	−66.3 (0.2)	−66.3 (0.2)	−62.6 (0.2)	−63.6 (0.2)	−65.0 (0.2)	−64.4 (0.2)	−66.7 (0.2)
	$E_{(total,\ GB)}$	543.5 (0.5)	549.6 (0.4)	546.7 (0.4)	554.0 (0.3)	552.2 (0.3)	549.8 (0.4)	555.7 (0.2)	554.3 (0.3)
	$\Delta E_{(total,\ GB)}$	**6.1**		**7.3**		**−3.4**		**−1.4**	
B	E_{electr}	−36.5 (0.1)	−48.5 (0.1)	−46.4 (0.1)	−48.6 (0.1)	−46.5 (0.1)	−46.5 (0.1)	−46.8 (0.1)	−48.6 (0.1)
	E_{vdW}	6.0 (0.0)	6.0 (0.0)	5.9 (0.0)	6.2 (0.0)	6.1 (0.0)	6.1 (0.0)	6.2 (0.0)	6.1 (0.0)
	$G_{(non\text{-}polar\ GB)}$	3.3 (0.0)	3.3 (0.0)	3.2 (0.0)	3.3 (0.0)	3.3 (0.0)	3.3 (0.0)	3.3 (0.0)	3.3 (0.0)
	G_{GB}	−11.4 (0.0)	−11.4 (0.0)	−11.4 (0.0)	−11.4 (0.0)	−11.5 (0.0)	−11.4 (0.0)	−11.3 (0.0)	−11.3 (0.0)
	$G_{solvation}$	−8.1 (0.0)	−8.2 (0.0)	−8.2 (0.0)	−8.1 (0.0)	−8.2 (0.0)	−8.1 (0.0)	−8.0 (0.0)	−8.0 (0.0)
	$E_{(total,\ GB)}$	−18.1 (0.1)	−29.5 (0.1)	−27.8 (0.1)	−28.2 (0.1)	−26.7 (0.1)	−27.2 (0.1)	−26.0 (0.1)	−28.5 (0.1)
	$\Delta E_{(total,\ GB)}$	**−11.4**		**−0.4**		**0.5**		**−2.5**	

The notation used for the four different penetration modes is that described in the text. The subindexes *R* and *S* have been added in order to make reference to the data obtained for **Ibu***R* and **Ibu***S*, respectively.
[a] Standard errors of the mean values.

Table 2. Energy contribution of the complex [**AB** ≡ **Ibu**(*R*,*S*)⊂β-CD]

	Energy (kcal/mol)	NP–W_R (std)[a]	NP–W_S (std)	P–W_R (std)	P–W_S (std)	NP–N_R (std)	NP–N_S (std)	P–N_R (std)	P–N_S (std)
AB	E_{electr}	399.8 (0.4)	392.3 (0.4)	396.5 (0.4)	388.0 (0.4)	394.1 (0.4)	394.0 (0.4)	393.4 (0.4)	392.1 (0.4)
	E_{vdW}	7.9 (0.3)	2.4 (0.3)	4.2 (0.3)	6.5 (0.3)	6.0 (0.3)	6.6 (0.3)	5.3 (0.3)	4.6 (0.3)
	$G_{(non\text{-}polar\ GB)}$	8.4 (0.0)	8.0 (0.0)	8.1 (0.0)	8.2 (0.0)	8.2 (0.0)	8.2 (0.0)	8.1 (0.0)	8.1 (0.0)
	G_{GB}	−78.9 (0.2)	−78.8 (0.2)	−81.6 (0.2)	−77.9 (0.2)	−79.3 (0.2)	−80.9 (0.2)	−78.4 (0.2)	−79.8 (0.2)
	$G_{solvation}$	−70.5 (0.2)	−70.9 (0.2)	−73.5 (0.3)	−69.7 (0.2)	−71.1 (0.2)	−72.7 (0.2)	−70.2 (0.3)	−71.7 (0.2)
	$E_{(total,\ GB)}$	508.8 (0.7)	499.7 (0.5)	501.0 (0.5)	509.0 (0.4)	508.7 (0.5)	506.0 (0.5)	511.5 (0.4)	506.7 (0.4)
	$\Delta E_{(total,\ GB)}$	**−9.1**		**8.0**		**−2.7**		**−4.8**	

[a] Standard errors of the mean values.

Table 3. Energy difference of the complex formation [$\Delta_{Binding}$ ≡ **AB** − (**A** + **B**)]

	Energy (kcal/mol)	NP–W_R (std)[a]	NP–W_S (std)	P–W_R (std)	P–W_S (std)	NP–N_R (std)	NP–N_S (std)	P–N_R (std)	P–N_S (std)
$\Delta_{Binding}$	E_{electr}	−2.7 (0.1)	−5.5 (0.1)	−1.5 (0.1)	−1.4 (0.1)	−1.3 (0.1)	−1.2 (0.1)	−3.2 (0.1)	−4.3 (0.1)
	E_{vdW}	−14.4 (0.3)	−18.5 (0.3)	−17.4 (0.3)	−16.5 (0.3)	−16.2 (0.3)	−15.9 (0.3)	−17.2 (0.3)	−17.8 (0.3)
	$G_{(non\text{-}polar\ GB)}$	−3.6 (0.0)	−4.0 (0.0)	−3.8 (0.0)	−3.8 (0.0)	−3.8 (0.0)	−3.8 (0.0)	−3.8 (0.0)	−3.8 (0.0)
	G_{GB}	4.1 (0.1)	7.6 (0.1)	4.8 (0.1)	4.8 (0.1)	4.5 (0.1)	4.1 (0.1)	6.0 (0.1)	6.8 (0.1)
	$G_{solvation}$	0.4 (0.1)	3.6 (0.2)	1.0 (0.1)	1.0 (0.1)	0.7 (0.1)	0.4 (0.1)	2.2 (0.1)	3.0 (0.1)
	$E_{(total,\ GB)}$	−16.6 (0.3)	−20.4 (0.2)	−17.9 (0.2)	−16.9 (0.2)	−16.8 (0.2)	−16.6 (0.2)	−18.2 (0.2)	−19.1 (0.2)
	$\Delta E_{(total,\ GB)}$	**−3.8**		**1.0**		**0.2**		**−0.9**	

[a] Standard errors of the mean values.

calculations suggest that the total chiral selectivity action by β-CD favors the **Ibu***S* enantiomer by about 0.9 kcal/mol. The computed average binding energies of −17.4 kcal/mol for the **Ibu***R* and of −18.3 kcal/mol for the **Ibu***S*, are about three times larger than the more recent experimentally available $\Delta G_{complex\_formation}$ data of −5.45 kcal/mol[22] and of −5.35 kcal/mol[23] for **Ibu** racemic mixtures.

The calculated $-T\Delta S$ values for the complexes [**Ibu***R*⊂β-CD] and [**Ibu***S*⊂β-CD] are 8.282 and 8.373 cal/mol, respectively. Thus the resulting $\Delta(T\Delta S)$ was too small to have an effective contribution to the overall $\Delta G_{binding}$ and it was not included in the present energy analysis. Recent thermodynamic studies on several enantiomeric pairs forming inclusion complexes with natural occurring CDs also report small differences on $\Delta\Delta S$ and $\Delta\Delta H$ in the overall complexation process.[35]

2.2. Hydrogen bond analysis

A full analysis of all possible hydrogen bonds formed between the primary or secondary hydroxyl groups of β-CD with the carboxylic group of **Ibu***R* and **Ibu***S* was carried out with the help of the PTRAJ subroutine of AMBER. For this analysis, the carboxyl group of **Ibu** was considered to act either as acceptor (through the CO or through the OH) or as donor (through the OH); similar properties were considered for the hydroxyl groups of β-CD. We used Jeffrey's hydrogen bond distance and bond angle criterion[36] to classify these from strong to weak hydrogen bonds. Table 4 compares the total number of hydrogen bonds present in all penetration modes studied.

Since the NP–W penetration mode was computed to contribute the most in the chiral selection process, only

Table 4. Hydrogen bonds formed per picosecond of simulation time during the complexation process for all penetration modes

			Moderate	Moderate + weak
NP–W		β-CD donor	0.40	1.21
	Ibu*R*	β-CD acceptor	0.06	0.46
		Total	**0.46**	**1.67**
		β-CD donor	0.73	1.88
	Ibu*S*	β-CD acceptor	0.08	0.56
		Total	**0.81**	**2.44**
P–W		β-CD donor	0.02	0.17
	Ibu*R*	β-CD acceptor	0.01	0.14
		Total	**0.03**	**0.31**
		β-CD donor	0.45	1.41
	Ibu*S*	β-CD acceptor	0.66 (0.48)[a]	1.04
		Total	**1.11 (0.92)**[a]	**2.45**
NP–N		β-CD donor	0.04	0.20
	Ibu*R*	β-CD acceptor	0.02	0.10
		Total	**0.06**	**0.30**
		β-CD donor	0.02	0.15
	Ibu*S*	β-CD acceptor	0.02	0.08
		Total	**0.04**	**0.23**
P–N		β-CD donor	0.50	1.42
	Ibu*R*	β-CD acceptor	0.11	0.64
		Total	**0.61**	**2.06**
		β-CD donor	0.56	1.56
	Ibu*S*	β-CD acceptor	0.14	0.64
		Total	**0.70**	**2.20**

[a] Number of H-bonds formed without considering the contacts with the O4 oxygen.

the results obtained in this arrangement are going to be described here. The results from the penetration modes and their intricate hydrogen bonding pattern formed during the simulation are discussed and depicted in the Supplementary material (Figs. 1–4).

In the NP–W penetration mode no strong hydrogen bonds were observed in any of the [**Ibu**(*R*,*S*)⊂β-CD] inclusion complexes, however, only moderate and weak H-bonds were detected. Upon further analysis, we observed that in both [**Ibu**(*R*,*S*)⊂β-CD] complexes the hydroxyl group on **Ibu** formed fewer hydrogen bonds than the corresponding carbonyl oxygen. Moreover, the first were classified as weak while the second were classified as moderate-weak. In most cases the hydrogen bonds were bifurcated between the hydroxyl groups of C3 and C2 of any glucose moiety.

Figure 1 of Supplementary material shows that more hydrogen bonds (moderate plus moderate-weak) were formed between the β-CD and the **Ibu*S*** enantiomer than with the **Ibu*R*** enantiomer in the NP–W penetration mode. The average number of total H-bonds in the [**Ibu*R*** ⊂β-CD] complex is 2.07 h bonds/ps while in the [**Ibu*S*** ⊂β-CD] complex the number raises up to 3.37 h bonds/ps; this is about 50% more hydrogen bonds than in the former. When moderate H-bonds are considered only, the difference between both isomers is even larger (about twice).

A sample of the hydrogen bonding trajectory is shown in Figure 3. This figure depicts the trajectory for the O···H distances between the carbonyl oxygen of **Ibu*S*** and the hydroxylic hydrogen corresponding to the OH in position 2 for any glucose residue in the NP–W penetration mode. This figure shows that the C═O forms a single H-bond with one of the secondary OH most of the simulation time, and that the H-bond position alternates between three different glucose units: two adjacent and a third one separated from the other two by one residue of glucose. After careful analysis of the geometries involving the H-bonds shown in this figure, we saw that they tend to be linear with O–H···O bond angles between 140 and 180° and H···O distances between 1.6 and 2.0 Å, these parameters are in agreement within those assigned to strong H-bonds. This analysis also indicates that when intermolecular H-bonds are formed between **Ibu** and the host, the intramolecular H-bonds between the O2 and O3 of β-CD are broken.

2.3. Trace of the chiral atom

The course followed by the chiral atom of **Ibu** in its corresponding [**Ibu**(*R*,*S*)⊂β-CD] complexes (hereinafter called trace) along the whole MD trajectory was computed with the help of the gOpenMol[37] program. The results for the trace in the NP–W inclusion mode are shown in Figure 4. The β-CD and corresponding **Ibu** isomer structure are the average structures computed over the 4500 ps of simulation, while the **Ibu** trace shown corresponds to the nonaveraged isomers and it is the trajectory of the chiral atom within the β-CD cavity.

The trace for **Ibu*R*** is more spherical than the one for **Ibu*S***. This is an indication that the latter has a more restricted motion within the CD cavity. The difference in the cavity volume explored by **Ibu** isomers is consistent with the results of the MM/GBSA and hydrogen bond analyses. Moreover, the average structure for the β-CD is more distorted in the [**Ibu*R*** ⊂β-CD] complex than in the

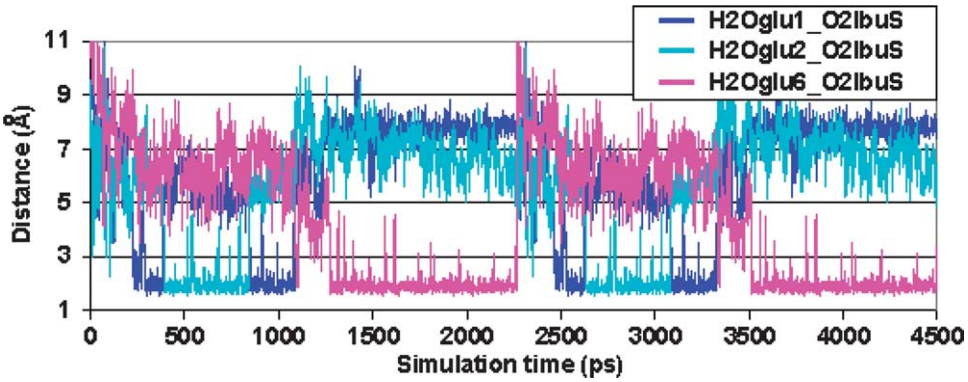

Figure 3. Distances between the carbonyl oxygen of **Ibu*S*** and the hydroxylic oxygen of the OH in position 2 for three specific glucose units.

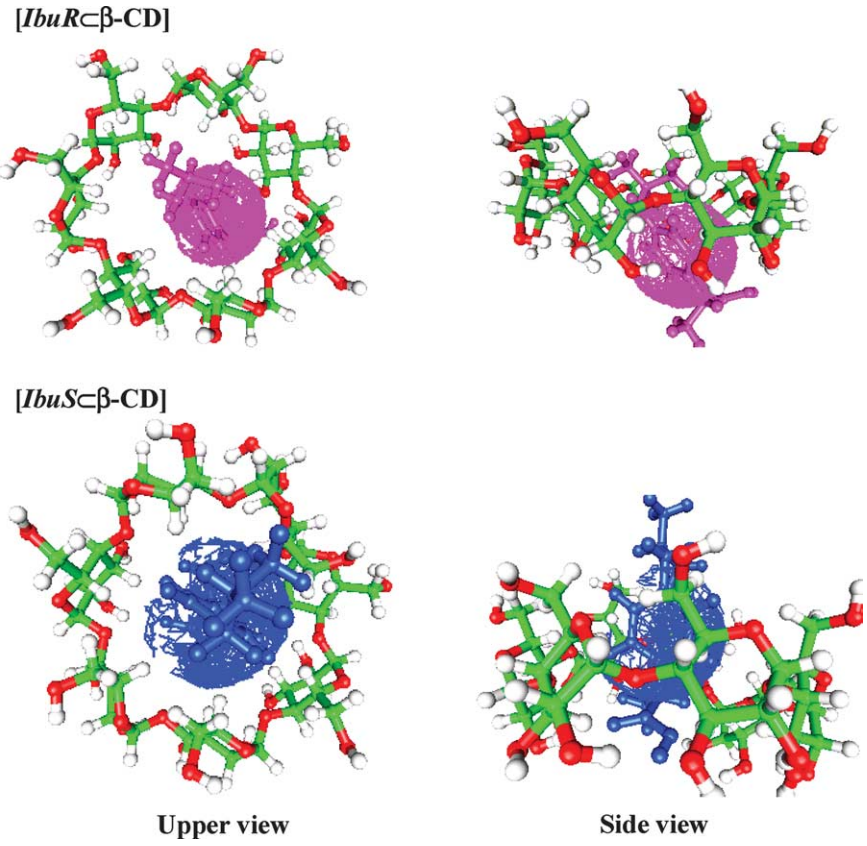

Figure 4. Trace followed by the chiral atom of **Ibu** in the [**Ibu***R*⊂β-CD] and [**Ibu***S*⊂β-CD] complexes in the NP–W arrangement in both upper and side view.

[**Ibu***S*⊂β-CD] one. Upon further observation, we saw that the first complex presents two glucose units that have lost their parallel arrangement and are tilted (with the secondary hydroxyls pointing towards the interior of the cavity), while the second complex presents only one of such tilted glucoses.

2.4. Structural features

In this section, we present the structural aspects for the average structures of the [**Ibu**(*R*,*S*)⊂β-CD] inclusion complexes as arising from 4.5 ns molecular dynamics simulations relative to available experimental thermodynamic and X-ray data.

All penetration modes formed a 1:1 inclusion complex in the first 10 ps of simulation, and they remained as such thereafter. However, in the P–W penetration mode an association complex was observed for the **Ibu***S* isomer. Since the energetic analysis shows the NP–W penetration mode as the most representative of the inclusion complexes formed (see Table 3), in Figure 5a and b we present the averaged structures of **Ibu***R* and **Ibu***S* as obtained from MOIL-View for this arrangement. The RMSd for the best fit of the non-minimized structures [**Ibu***R*⊂β-CD] versus [**Ibu***S*⊂β-CD] and the corresponding minimized structures are 2.042 and 1.867, respectively. The superimposition of the non-minimized and minimized structures of **Ibu***R* is shown in Figure 5c and the corresponding structures of **Ibu***S* in Figure 5d. The RMSd for their best fit are 0.9615 and 0.7524, respectively. It is noteworthy that after minimization, in the absence of explicit solvent, **Ibu***R* moves into the β-CD cavity where the aromatic ring and the polar group suffer a better orientation due to electrostatics, while **Ibu***S* suffers minor geometric adjustments. The preferred NP–W penetration mode of **Ibu** inclusion correlates well with ^{1}H NMR results.[28b] Moreover, in similar solvent, temperature and pH conditions our simulation predicts the correct elution order of the enantiomers in capillary electrophoresis experiments.[26a]

A recent crystallographic study of the inclusion complex between pure **Ibu***S* and β-CD[25] presents a 2:1 host–guest stoichiometry in a head-to-head dimer, where the carboxylic end of the **Ibu***S* molecule faces the narrower rim of β-CD, position further stabilized by a hydrogen bond with one of the primary hydroxyl groups of the host. This mode of inclusion is opposite to the one we report and to the ^{1}H NMR results.[28b] The disagreement might originate because our simulations correspond to a solvated inclusion complex in a 1:1 host–guest stoichiometry, while in the crystal structure the formation of a 2:1 host–guest stoichiometry favors a channel type structure that could give extra stability to the **Ibu***S* orientation. Since the crystallographic structure does not indicate the direction of inclusion, we hypothesize that only the P–W and NP–N penetration modes could favor this orientation.

2.5. Electronic absorption data

Ibuprofen forms 1:1 inclusion complexes with α, β and γ cyclodextrins, in pH 7.5 buffer aqueous solutions. The interaction constant of [**Ibu**$^{-1}$⊂β-CD] at 298 K is

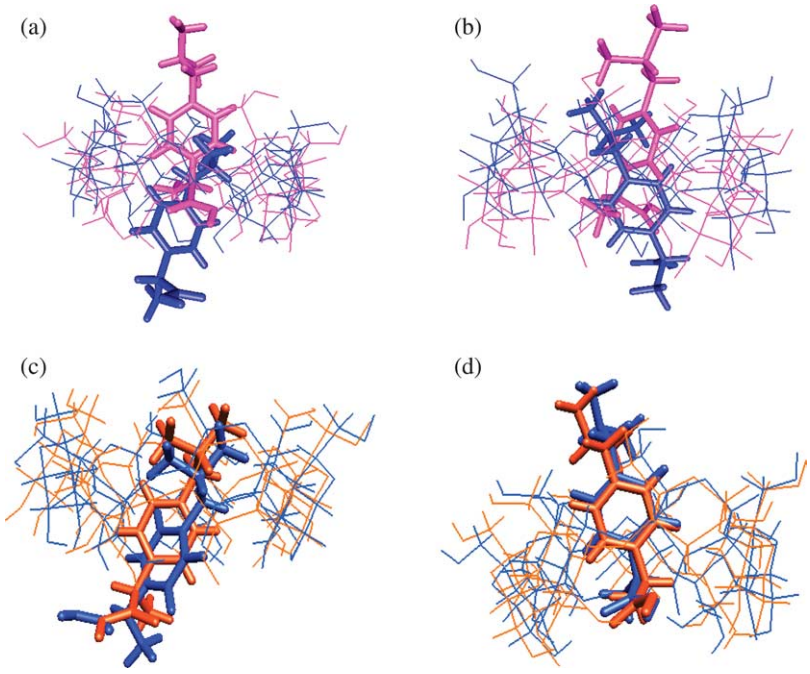

Figure 5. Average structures of the [**Ibu***R*⊂β-CD] and [**Ibu***S*⊂β-CD] complexes after 4.5 ns of simulation of the initial NP–W arrangement. (a) Nonminimized structures, in blue that of the **Ibu***R* enantiomer and in magenta that of the **Ibu***S* enantiomer. (b) Minimized structures of the same complexes shown in (a). (c) Comparison of the nonminimized (blue) and minimized (orange) average structure of [**Ibu***R*⊂β-CD]. (d) Comparison of the nonminimized (blue) and minimized (orange) average structure of [**Ibu***S*⊂β-CD].

$170\pm10\ M^{-1}$; some of its thermodynamic parameter values were determined: $\Delta H_{interaction}$ and $\Delta S_{interaction}$, $+2.82$ kcal mol^{-1} and $+0.019$ kcal mol^{-1} K^{-1}, respectively. While the values of the corresponding interaction constants for [**Ibu**$^{-1}$⊂α-CD] and [**Ibu**$^{-1}$⊂γ-CD] complexes, under the same reaction conditions, are: 190 ± 10 and $170\pm15\ M^{-1}$, respectively.[38] Therefore, the magnitude of these interaction constants for the 1:1 complexes seems to indicate that the cavity size of the cyclodextrins is not an important factor for the **Ibu** complexation. Additionally, these interaction constants are small in comparison with other reported values for anti-inflammatory-cyclodextrin binding constants.[39] There are several reports[40] in the literature about the complexation of guest molecules containing alkyl chains and cyclodextrins, where the alkyl moieties are included into the cyclodextrin cavity; in these cases the binding constants are also small.

2.6. Two dimensional NMR spectra

The alkyl chain of **Ibu** is part of its hydrophobic moiety involved in the complexation. The negatively charged group of this guest species drives the direction in which it is oriented during the inclusion process. The carboxylate group remains in contact with the aqueous solution and the uncharged moiety is included in the cyclodextrin cavity.

The NOESY spectrum (see Fig. 5 of the Supplementary material) shows changes corresponding to the signals of H-3 of the β-CD. Significant changes in the corresponding signals of the H-2 and H-4 are also observed on cyclodextrin external protons. This NOESY spectrum is indication of a weak interaction between the **Ibu** molecule and the β-CD. Both, the aromatic and the alkyl moieties are included into the cyclodextrin ring and are protected from the aqueous solution and the β-CD hydroxylic groups. The interaction of the guest with H-3, localized in the interior of the β-CD cavity and close to its wide part, and is due to the *iso*-alkyl group and the aromatic ring, when **Ibu** is included. The *iso*-butyl chain is completely included; however, the characteristic band associated with the interaction of H-5 of β-CD is absent in this spectrum. Perhaps, the great difference between the *iso*-butyl chain size and the internal cyclodextrin diameter, (≈4.3 and 7.8 Å, respectively) is responsible for this weak interaction.

The β-CD external section is also affected by the interaction with the *iso*-butyl chain of the guest molecule. When the [**Ibu**$^{-1}$⊂β-CD] complex is formed the *iso*-butyl chain is completely included, the –CH_2 group and the benzene ring remain close to H-5 and H-3, respectively. However, only the interaction with H-3 can be inferred in this spectrum, since the ibuprofen –CH_2 group weakly interacts with the internal H-5 of the host molecule.

The –CH group of the *iso*-butyl chain displays a small interaction signal with the H-6 of the β-CD, the remaining methyl and C-H groups of the guest that are not included within the confinement of the cyclodextrin, interact with the host external hydrogen atoms.

It can be suggested that the small interaction constant values is due to the small surface contact between the guest and host molecules, since ibuprofen is small for the cavity.

3. Conclusions

The main driving forces for complexation are dominated by non-bonded van der Waals intermolecular interactions and

the non-polar contributions to solvation, although the relative orientation of the interacting molecules and the presence of topical H-bonds between the polar part of the drug and the OH groups of the β-CD rims play a further role in stabilizing the supramolecular assemblies. Calculations of the energy components showed that under the conditions considered all 1:1 inclusion complexes are stable and, that a preferential way of insertion was detected, exception made for **Ibu***S* in the P–W penetration mode in which an association complex was formed.

The preferred penetration mode found corresponds to a geometry where the non-polar group of **Ibu** faces the wider cavity of the β-CD (NP–W). In this geometry, the **Ibu***R* enantiomer moves more freely inside the host cavity after insertion, while the **Ibu***S* enantiomer presents a more restricted motion. Moreover, the **Ibu***S* enantiomer forms a significant number of moderate to strong hydrogen bonds with the secondary hydroxyl groups of β-CD during the entire simulation time, while the **Ibu***R* enantiomer does not present such feature. In general, the energetic analysis reveals that the **Ibu***S* enantiomer is about 1 kcal/mol more tightly bonded than the **Ibu***R* enantiomer. This rather small energy difference is not enough to explain the chiral selectivity shown by β-CD upon **Ibu** isomers, however, the apparent geometrical differences shown by the [**Ibu**(*R*,*S*)⊂β-CD] molecular complexes suggest that the **Ibu** chiral discrimination is also due to an induced fit effect.

In summary, we have shown that the recognition process is based upon four steps. Step1: formation of the guest–host complex. Step 2: positioning of both guest and host to optimize interactions (conformational adjustments). Step 3: formation of secondary interactions (activation of the complexes). Step 4: expression of molecular fit (chiral recognition). Within the limits of this study we did not detect any three-point recognition process.

The small contact surface formed from the inclusion complexes of $\mathbf{Ibu}^{-1}$ ion and the cyclodextrin cavity discards van der Waals interactions as a stabilizing factor of the inclusion complex. The positive values of the $\Delta H_{\text{interaction}}$ and $\Delta S_{\text{interaction}}$, computed from the absorption electronic spectroscopic data, lead to the identification of the hydrophobic effect as the driving force for the formation of the [$\mathbf{Ibu}^{-1}$⊂β-CD] complex in aqueous solution; while the geometry of this inclusion complex was established by the $\text{ion}_{\text{ibuprofen}}$–$\text{dipole}_{\beta\text{-CD}}$ interaction. The $\mathbf{Ibu}^{-1}$ ion produces 1:1 inclusion complexes with the smallest interaction constant values, when compared with other anti-inflammatory-cyclodextrin complexes.

4. Construction of models

The atomic coordinates for the *S*-(+)-**Ibu** enantiomer (**Ibu***S*) were obtained from the 3D Pharmaceutical Structure Database (3DPSD).[41] The *R*-(−)-**Ibu** enantiomer (**Ibu***R*) was obtained from reflection of the first one. The β-CD molecule was built using the PREP/LINK/EDIT/PARM modules of the AMBER v.5 programs[42] suite, by connecting seven D-glucopyranose units from the GLYCAM_93 fragment library[43] through the α-(1,4) glycosidic linkages.

The starting orientations for the inclusion complexes were built by the combination of all the insertion possibilities, thereby identified as the penetration modes NP–W, NP–N, P–W and P–N shown in Figure 2. For instance, NP–W means that the non-polar chain of **Ibu** is placed at the entrance of the wide rim, or secondary hydroxyl rim, of β-CD. The rest of the labels are self explanatory.

The 1:1 inclusion complexes were constructed between β-CD and each one of the two **Ibu** enantiomers in the neutral moiety. The corresponding geometries were achieved with the aid of the docking module of the InsightII program package.[44] Unfavorable interactions within these structures were relieved by energy minimization with steepest descent followed by conjugate gradient energy minimization until the RMS of the elements of the gradient vector was less than 10^{-4} kcal/(mol Å).

5. Computational methodology

The parm94 force field,[45] the GLYCAM_93[43] set of parameters and the AMBER program[42] were used throughout this work. The partial atomic charges for the neutral **Ibu** isomers were obtained following the RESP methodology.[46] Accordingly, four low energy conformations of each **Ibu** enantiomer were minimized with the DFT method (B3LYP/6-31G**)[47] implemented in the Jaguar program,[48] and the electrostatic potential (ESP) was calculated at the HF/6-31G* level. For a better estimation of the guest atomic charges in the hydrophobic interior of β-CD, the ESP mesh was computed as if the **Ibu** molecule was immersed in cyclohexane. This was accomplished using the corresponding solvation module of Jaguar. In these calculations the solute is represented by a set of atomic charges and the solvent as a layer of charges at the solute molecular surface. The final set of atomic charges used in these computations is the result of averaging a total of eight conformations (four for each enantiomer). The atomic charges for β-CD were taken from the literature.[43]

The 1:1 inclusion complexes were solvated by a cubic box of 35 Å per side of TIP3P[49] water molecules, equivalent to a 0.001 M solution of pH 4.5. These conditions resemble those reported on capillary electrophoresis experiments.[50,51] The water imbibed models were gradually heated from 0 to 300 K in three steps of 100 K each. Each step had duration of 5 ps with diminishing restrains for the solute. The full system with no-restrains was equilibrated for approximately 20 ps at 300 K. This was followed by 4500 ps of data collection runs in order to examine the complex dynamics and structure. The temperature was maintained at 300 K by the Berendsen coupling algorithm,[52] with separate solute–solvent and solvent–solvent coupling. A total of 4500 snapshots were saved during the data collection period, one snapshot per 1 ps of MD simulation. Visual inspection showed that the 1:1 inclusion complex was formed within the first picoseconds of simulation and that it was stable during the entire simulation period. In order to compare with experimental results, various physical properties associated with the host molecule were calculated using the various modules present in the AMBER v.5 suite of programs.[42]

The MD simulations were carried out under an NPT ensemble. Periodic boundary conditions with a primary cutoff of 9 and 15 Å for a secondary cutoff for non-bonded interactions were applied. The long range electrostatic interactions were evaluated by the Ewald method.[53] The leap-frog algorithm with a time step of 1 fs with sampling taken every 1 ps was used. SHAKE was used for all bonds containing hydrogens.[54]

To estimate the binding free energy on the complex formation we employed the MM-PBSA/GBSA methodology[14,55,56] since it has been successfully applied to study the binding of small druglike molecules[57,58] to proteins,[59,60] RNA[61] and DNA.[16] In the frame of this methodology the free energy of binding for the association reaction A + B → AB is calculated using the following thermodynamic cycle:

$$\begin{array}{ccccc} A_{aqu} & + & B_{aqu} & \xrightarrow{\Delta G_{binding}} & AB_{aqu} \\ \downarrow{\scriptstyle -\Delta G^{A}_{solv}} & & \downarrow{\scriptstyle -\Delta G^{B}_{solv}} & & \downarrow{\scriptstyle \Delta G^{AB}_{solv}} \\ A_{gas} & + & B_{gas} & \xrightarrow{\Delta G_{gas}} & AB_{gas} \end{array}$$

$$\begin{aligned} \Delta G_{\text{binding}} &= \Delta G_{\text{gas}} - \Delta G^{\text{A}}_{\text{solv}} - \Delta G^{\text{B}}_{\text{solv}} + \Delta G^{\text{AB}}_{\text{solv}} \\ &= \Delta H_{\text{gas}} - T\Delta S - \Delta G^{\text{A}}_{\text{GBSA}} - \Delta G^{\text{B}}_{\text{GBSA}} + \Delta G^{\text{AB}}_{\text{GBSA}} \end{aligned}$$

where ΔG_{gas} is the interaction energy between A and B in the gas phase and $\Delta G^{\text{A}}_{\text{solv}}$, $\Delta G^{\text{B}}_{\text{solv}}$ and $\Delta G^{\text{AB}}_{\text{solv}}$ are the solvation free energies of A, B and AB, which are estimated using a continuum approach, that is, $\Delta G^{\text{A}}_{\text{solv}} = \Delta G^{\text{A}}_{\text{GBSA}} = \Delta G^{\text{A}}_{\text{GB}} + \Delta G^{\text{A}}_{\text{SA}}$, etc. Therefore,

$$\Delta G_{\text{binding}} = \Delta H_{\text{gas}} - T\Delta S + \Delta\Delta G_{\text{GB}} + \Delta\Delta G_{\text{SA}}$$

where

$$\Delta H_{\text{gas}} \approx \Delta E_{\text{gas}} = \Delta E_{\text{intra}} + \Delta E_{\text{electrostatic}} + \Delta E_{\text{vdw}} = E_{\text{MM}}$$

and

$$\Delta\Delta G_{\text{GB}} = \Delta G^{\text{AB}}_{\text{GB}} - \left(\Delta G^{\text{A}}_{\text{GB}} + \Delta G^{\text{B}}_{\text{GB}}\right)$$

$$\Delta\Delta G_{\text{SA}} = \Delta G^{\text{AB}}_{\text{SA}} - \left(\Delta G^{\text{A}}_{\text{SA}} + \Delta G^{\text{B}}_{\text{SA}}\right)$$

The polar solvation energy contribution is computed in continuum solvent with the Generalized Born (G_{GB}) model using the PARSE van der Waals radii,[62] with interior and exterior dielectric constants of 1 and 80, respectively; while the non-polar solvation energy contribution or the solvent accessible surface area (SASA) for each isolated state (host, guest, or complex) is calculated as $G_{\text{SA}} = \gamma\text{SA} + b$, where $\gamma = 0.00542$ kcal/(mol Å^2) and $b = 0.92$ kcal/mol, and SA is estimated with the MSMS program.[63]

The change of solute entropy upon binding, $-T\Delta S$, was estimated using the NMODE module of AMBER and the MOIL-View program[64] v.10.0. With MOIL-View we performed a cluster analysis of the [**Ibu**(*R*,*S*)⊂β-CD] complex structures within a RMSD of 1 Å during the MD trajectories. We focused on the six most populated clusters and obtained an average structure for each one of these clusters. These structures were minimized using a distance dependent dielectric constant of $\varepsilon = 4r_i$, to account for solvent screening, and its entropy was calculated using classical statistical formulas and normal mode analysis.

We also assumed that if one wishes to calculate the binding free energy difference between two similar guests bound to the same host, this process can be described by the following thermodynamic cycle:

$$\begin{array}{ccccc} IbuR & + & \beta CD & \xrightarrow{\Delta G^{R}_{binding}} & IbuR:\beta\ CD \\ \downarrow{\scriptstyle \Delta G_{solv}} & & & & \downarrow{\scriptstyle \Delta G_{B}} \\ IbuS & + & \beta\ CD & \xrightarrow{\Delta G^{S}_{binding}} & IbuS:\beta\ CD \end{array}$$

In such a way that,

$$\Delta\Delta G = \Delta G^{\text{R}}_{\text{binding}} - \Delta G^{\text{S}}_{\text{binding}} = \Delta G_{\text{solv}} - \Delta G_{\text{B}},$$

where $\Delta G^{\text{R}}_{\text{binding}}$ and $\Delta G^{\text{S}}_{\text{binding}}$ are the binding free energies for the R and S isomers of **Ibu**, respectively, and ΔG_{solv} and ΔG_{B} are the nonphysical transmutation free energy from the *R* to the *S* isomer of **Ibu** in free and bound states. Since we are interested in learning about the structural and energetic features that lead to chiral discrimination, we propose that we can calculate the binding free energy difference of the two enantiomers as $\Delta\Delta G = \Delta G^{\text{R}}_{\text{binding}} - \Delta G^{\text{S}}_{\text{binding}}$, where the $\Delta G_{\text{binding}}$ is calculated using the MM/GBSA methodology as described above. The ensemble of structures was generated by sampling the MD trajectory every 4 ps.

The hydrogen bond analysis was done with the hbond subroutine the PTRAJ module of AMBER. The maximum distance between acceptor oxygen and donor oxygen was considered to be 4.05 Å, and resulting hydrogen bonds were classified as strong, moderate and weak according to Jeffrey.[36]

AMBER MD calculations were performed on a SGI Onix R4400 with OS IRIX 6.5 and the MM/GBSA calculations were carried out in a PC Pentium III computer with Linux v.7.1.

6. Experimental

6.1. Chemical reagents

Ibuprofen (Boehringer-Ingelheim Promeco laboratories, Mexico City); β-CD was a donation from Arancia Mexico. The buffer components, Na_2HPO_4 and KH_2PO_4, and D_2O (99.9 at.% D) were supplied by Aldrich. NaCl, R.A. was purchased from Mallinckrodt. Water was distilled in a Barnstead Thermolyne System and given a second treatment in the Easypure RF Compact Ultrapure Water System. All chemical reagents were used without further purification except for β-CD. A 2% aqueous solution of β-CD was left to stand at room temperature for a long time in order to promote aggregation of insoluble impurities and complexes; the solution was then filtered off before recrystallization. β-CD was recrystallized from boiling water and it was then rinsed several times with ethanol, acetone and cold water.[65]

6.2. Preparation of the inclusion complexes

Prior to the inclusion complex study, we prepared a series of ibuprofen solutions in the calculated concentration range in aqueous solution to generate a calibration curve. The calibration curve was used to determine the absorbance of the guest at 10^{-5} mol dm^{-3}. In aqueous solution, the absorbance of β-CD in the concentration range studied (10^{-3}–10^{-2} mol dm^{-3}) was also known. Inclusion compounds were prepared by direct dissolution. The 10^{-5} mol dm^{-3} guest solutions were employed to dissolve increasing concentrations of cyclodextrin. In this way, the inclusion compound solutions were prepared. The buffer solution, pH 7.5, consists of Na_2HPO_4/KH_2PO_4 (0.07895 mol dm^{-3}) with constant ionic strength of 0.1 mol dm^{-3} NaCl. At this pH the carboxylic group of ibuprofen takes the ionic form of the ibuprofenate ion (**Ibu**$^{-1}$).

The absorption spectra of each solution series were measured 24 h after their preparation using a 1 cm path length cell. Each solution was measured several times. Thus, the resulting absorption data are average values, to minimize the measurement errors. The same general procedure was followed for the formation of inclusion complexes in the other reaction media.

6.3. Spectroscopic measurements

The UV–vis electronic absorption spectra were determined using a Hewlett Packard 8452A Diode Array Spectrophotometer. The temperature was kept constant by means of a Peltier Hewlett Packard 89090A system. Water was used as blank in all measurements.

^{1}H NMR experiments were carried out in non-buffered D_2O solutions. 1D ^{1}H NMR spectra were collected on a 300 MHz Varian Unity Plus spectrometer using a frequency of 299.95 MHz, with a 45° pulse (6.7 μs), spectral width of 3229.5 Hz, 3.002 s of acquisition time and 298 K. The number of transients acquired (32–128) depended on the sample sensitivity. Nuclear Overhauser Effect (NOESY) data were collected with the same 300 MHz Varian Unity Plus spectrometer, with a broad band switchable probe. Spectral width was 2731.5 Hz in both dimensions, with an acquisition time of 0.187 s.

Acknowledgements

We acknowledge the financial support from the Mexican Council for Science and Technology (CONACyT 25245-E to R.G.J.), from the National University of Mexico (UNAM-PAPIIT IN109999 and IN107701 to R.G.J., and UNAM-PAPIIT IN203391 to D.D.), and from the Spanish Ministry of Science and Technology (PPQ2000-0369 to C.J.). Supercomputing time was gratuitously provided by DGSCA-UNAM. We acknowledge Dr. G. Mendoza-Díaz for the NMR spectra records and to Arancia Mexico and Cerestar USA Inc. for providing the cyclodextrins. This work is part of C.J.N.A.'s Master in Science Thesis and thanks CONACyT and PAPIIT-UNAM for graduate fellowships. C.M.E.L. thanks DGAPA-UNAM for a Ph.D. fellowship.

Supplementary data

Supplementary data associated with this article can be found, in the online version, at doi:10.1016/j.tet.2006.02.010. Distribution of the hydrogen bonding pattern of the NP–W, P–W and P–N penetration modes, the average structure of the **Ibu***S*:β-CD association complex as obtained from the MD for the P–W arrangement, and the NOESY spectrum of the [**Ibu**$^{-1}$⊂β-CD] complex in D2O at 298 K are given.

References and notes

1. Podlech, J. *Cell. Mol. Life Sci.* **2002**, *58*, 44–60.
2. Li, S.; Purdy, W. C. *Anal. Chem.* **1992**, *64*, 1405–1412.
3. Schneider, H.-J.; Hacket, F.; Rüdiger, V. *Chem. Rev.* **1998**, *98*, 1755–1785.
4. Kano, K.; Kamo, H.; Negi, S.; Kitae, T.; Takaoka, R.; Yamaguchi, M.; Okubo, H.; Hirama, M. *J. Chem. Soc., Perkin Trans. 2* **1999**, 15–21.
5. Rekharsky, M. V.; Inoue, Y. *Chem. Rev.* **1998**, *98*, 1875–1917.
6. Matchett, M. W.; Branch, S. K.; Jefferies, T. M. *Chirality* **1996**, *8*, 126–130.
7. Redondo, J.; Blázquez, M. A.; Torrens, A. *Chirality* **1999**, *11*, 694–700.
8. He, H.; Liu, Y.; Sun, C.; Wang, X.; Pham-Huy, C. *J. Chromatogr. Sci.* **2004**, *42*, 62–66.
9. Tazerouti, F.; Badjah-Hadj-Ahmed, A. Y.; Meklati, B. Y.; Franco, P.; Minguillon, C. *Chirality* **2002**, *14*, 59–66.
10. Nie, M. Y.; Zhou, L. M.; Wang, Q. H.; Zhu, D. Q. *Anal. Sci.* **2001**, *17*, 1183–1187.
11. Salvatierra, D.; Jaime, C.; Virgili, A.; Sánchez-Ferrando, F. *J. Org. Chem.* **1996**, *61*, 9578–9581.
12. Lipkowitz, K.; Stoehr, C. M. *Chirality* **1996**, *8*, 341–350.
13. Salvatierra, D.; Sánchez-Ruiz, X.; Garduño-Juárez, R.; Cervelló, E.; Jaime, C.; Virgili, A.; Sánchez-Ferrando, F. *Tetrahedron* **2000**, *56*, 3035–3041.
14. Srinavasan, J.; Cheatham, T. E.; Cieplak, P.; Kollman, P. A.; Case, D. A. *J. Am. Chem. Soc.* **1998**, *120*, 9401–9409.
15. Gouda, H.; Kuntz, I. D.; Case, D. A.; Kollman, P. A. *Biopolymers* **2003**, *68*, 16–34.
16. Trieb, M.; Rauch, C.; Wibowo, F. R.; Wellenzohn, B.; Leidl, K. B. *Nucleic Acids Res.* **2004**, *32*, 4696–4703.
17. Rizzo, R. C.; Toba, S.; Kuntz, I. D. *J. Med. Chem.* **2004**, *47*, 3065–3074.
18. Dalgliesh, C. E. *J. Chem. Soc.* **1952**, 3940–3952.
19. Booth, T. D.; Wahnon, D.; Wainer, I. W. *Chirality* **1997**, *9*, 96–98.
20. Kafri, R.; Lancet, D. *Chirality* **2004**, *16*, 369–378.
21. Bhushan, R.; Martens, J. *Biomed. Chromatogr.* **1998**, *12*, 309–316.
22. Mura, P.; Bettinetti, G. P.; Manderioli, A.; Faucci, M. T.; Bramanti, G.; Sorrenti, M. *Int. J. Pharm.* **1998**, *166*, 189–203.

23. Manzoori, J.; Amjadi, M. *Spectrochimica Acta* **2003**, *59*, 909–916.
24. Hergert, L. A.; Escandar, G. M. *Talanta* **2003**, *60*, 235–246.
25. Braga, S. S.; Goncalves, I. S.; Herdtweck, E.; Teixeira-Días, J. J. C. *New J. Chem.* **2003**, *27*, 597–601.
26. (a) Rawjee, Y. Y.; Staerk, D. U.; Vigh, G. *J. Chromatogr.* **1993**, *635*, 291–306. (b) Végvári, A.; Földesi, A.; Hetényi, C.; Kocnegarova, O.; Schmid, M. G.; Kudirkaite, V.; Stellan, H. *Electrophoresis* **2000**, *21*, 3116–3125. (c) Magnusson, J.; Blomberg, L. G.; Claude, S.; Tabachi, R.; Saxer, A.; Schürch, S. *J. High Resolut. Chromatogr.* **2002**, *23*, 619–627. (d) Abushoffa, A. M.; Fillet, M.; Hubert, P.; Crommen, J. *J. Chromatogr. A* **2002**, *948*, 321–329. (e) Perrin, C.; Vander, H.; Yvan, M.; Maftouh, M.; Massart, D. L. *Electrophoresis* **2001**, *22*, 3203–3215.
27. Junquera, E.; Martin-Pastor, M.; Aicart, E. *J. Org. Chem.* **1998**, *63*, 4349–4358.
28. (a) Oh, I.; Lee, M. Y.; Lee, Y. B.; Shin, S. C.; Park, H. *Int. J. Pharm.* **1998**, *175*, 215–223. (b) Ghorab, M. K.; Adeyeye, M. C. *Pharm. Dev. Technol.* **2001**, *6*, 315–324.
29. Johannsen, M. *J. Chromatogr. A* **2001**, *937*, 135–138.
30. Faucci, M. T.; Melani, F.; Mura, P. *Chem. Phys. Lett.* **2002**, *358*, 383–390.
31. Cao, Y.; Xiao, X.; Lu, R.; Guo, Q. *J. Inclusion Phenom. Macrocycl. Chem.* **2003**, *46*, 195–200.
32. Bergeron, R. J.; Channing, M. A.; McGovern, K. A. *J. Am. Chem. Soc.* **1978**, *100*, 2878.
33. Simova, S.; Schneider, H.-J. *J. Chem. Soc., Perkin Trans. 2* **2000**, 1717–1722.
34. Aree, T.; Chaichit, N. *Carbohydr. Res.* **2003**, *328*, 439–446.
35. Rekharsky, M.; Inoue, Y. *J. Am. Chem. Soc.* **2000**, *122*, 4418–4435.
36. Jeffrey, G. A. *The Hydrogen Bonding*; Oxford University Press: New York, 1997; Chapter 1, p 2.
37. Bergman, D. L.; Laaksonen, L.; Laaksonen, A. *J. Mol. Graphics Modell.* **1997**, *15*, 301–306.
38. Escobar-Llanos M. C. Ph.D. Thesis. UNAM, Mexico, 1998, pp 70–76.
39. (a) Escobar-Llanos, C. M.; Díaz, D.; Mendoza-Díaz, G. *J. Inclusion Phenom. Mol. Recognit. Chem.* **1998**, *31*, 333–349. (b) Diaz, D.; Escobar-Llanos, M. C.; Bernad-Bernad, M. J. *Drug Dev. Ind. Pharm.* **1999**, *25*, 107–115. (c) Diaz, D.; Escobar-Llanos, C. M.; Bernad-Bernad, M. J.; Gracia-Mora, J. *Pharm. Dev. Technol.* **1998**, *3*, 307–314.
40. (a) Gelb, R. I.; Schartz, L. M. *J. Inclusion Phenom. Mol. Recognit. Chem.* **1989**, *7*, 465. (b) Král'ova, K.; Mitterhauszerová, L. *Acta Chim. Hung.* **1992**, *129*, 885. (c) Buvári, A.; Szejtli, J.; Barcza, L. *J. Inclusion Phenom. Mol. Recognit. Chem.* **1983**, *1*, 151. (d) Tee, O. S.; Gadosy, T. A.; Giorgi, J. B. *J. Chem. Soc., Perkin Trans. 2* **1993**, 1705–1706.
41. http://www.ps.toyaku.ac.jp/dobashi/3dpsd/index.htm.
42. Case, D. A.; Pearlman, D. A.; Caldwell, J. W.; Cheatham, T. E., III; Ross, W. S.; Simmerling, C. L.; Darden, T. A.; Merz, K. M.; Stanton, R. V.; Cheng, A. L.; Vincent, J. J.; Crowley, M.; Ferguson, D. M.; Radmer, R. J.; Seibel, G. L.; Singh, U. C.; Weiner, P. K.; Kollman, P. A. *AMBER 5*; University of California: San Francisco, 1995.
43. (a) Woods, R. J.; Dwek, R. A.; Edge, C. J.; Fraser-Reid, B. *J. Phys. Chem.* **1995**, *99*, 3832–3846. (b) http://glycam.ccrc.uga.edu/glycam/gl_params.html.
44. InsightII (versión 97.0) is distributed by BIOSYM Technologies Inc.: 9685 Scranton Road, San Diego, CA 92121-2777.
45. Cornell, W. D.; Cieplak, P.; Bayly, C. I.; Gould, I. R.; Merz, K. M.; Ferguson, D. M.; Spellmeyer, D. C.; Fox, T.; Caldwell, J. W.; Kollman, P. A. *J. Am. Chem. Soc.* **1995**, *117*, 5179–5197.
46. Bayly, C. I.; Cieplak, P.; Cornell, W. D.; Kollman, P. A. *J. Phys. Chem.* **1993**, *97*, 10269–10280.
47. Becke, A. D. *J. Chem. Phys.* **1993**, *98*, 1372–1377.
48. *Jaguar*, version 3.5, Schrödinger Inc.: Portland OR, 1998.
49. Jorgensen, W. L.; Chandrasekhar, J.; Madura, J. D.; Impey, R. W.; Klein, M. L. *J. Chem. Phys.* **1983**, *79*, 926–930.
50. Reijenga, J. C.; Ingelse, B. A.; Everaerts, F. M. *J. Chromatogr. A.* **1997**, *792*, 371–378.
51. Blanco, M.; Ciello, J.; Iturriaga, H.; Maspoch, S.; Pérez-Maseda, C. *J. Chromatogr. A.* **1998**, *793*, 165–175.
52. Berendsen, H. J. C.; Postma, J. P. M.; van Gunsteren, W. F.; DiNola, A.; Haak, J. R. *J. Comput. Phys.* **1984**, *81*, 3684–3690.
53. Allen, M. P.; Tildesley, D. J. *Computer Simulation of Liquids*; Clarendon: Oxford, 1987.
54. van Gunsteren, W. F.; Berendsen, H. J. C. *Mol. Phys.* **1977**, *34*, 1311.
55. Kollman, P. A.; Massova, I.; Reyes, C.; Kuhn, B.; Huo, S.; Chong, L.; Lee, M.; Lee, T.; Duan, Y.; Wang, W.; Donini, O.; Cieplak, P.; Srinivasan, J.; Case, D. A.; Cheatham, T. E. *Acc. Chem. Res.* **2000**, *33*, 889–897.
56. Massova, I.; Kollman, P. A. *Perspect. Drug Discov. Des.* **2000**, *18*, 113–135.
57. Zou, X.; Sun, Y.; Kuntz, I. D. *J. Am. Chem. Soc.* **1999**, *121*, 8033–8043.
58. Choi, Y.; Jung, S. *Carbohydr. Res.* **2004**, *339*, 1961–1966.
59. Lee, M. R.; Duan, Y.; Kollman, P. A. *Proteins: Struct. Funct. Genet.* **2000**, *39*, 309–316.
60. Bryce, R. A.; Hiller, I. H.; Hismith, J. H. *Biophys. J.* **2001**, *81*, 1373–1388.
61. Reyes, C. M.; Kollman, P. A. *J. Mol. Biol.* **2000**, *295*, 1–6.
62. Sitkoff, D.; Sharp, K. A.; Honig, B. *J. Phys. Chem.* **1994**, *98*, 1978–1988.
63. Sanner, M. F.; Olson, A. J.; Spehner, J. C. *Biopolymers* **1996**, *38*, 305–320.
64. Simmerling, C.; Elber, R.; Zhang, J. In *Modeling of Biomolecular Structure and Mechanisms*; Pullman, A. et al, Ed.; Kluwer: Netherlands, 1995; pp 241–265.
65. Sophianopoulos, A. J.; Warner, I. M. *Anal. Chem.* **1992**, *64*, 2652–2654.